Geophys. J. Int. (1992) 110, 577–590

A mathematical model for compaction in sedimentary basins

D.M. Audet and A.C. Fowler

Centre for Industrial and Applied Mathematics, Mathematical Institute, Oxford University, 24–29 St Giles', Oxford OX1 3LB

Accepted 1992 March 26. Received 1991 July 8

SUMMARY

A mathematical model for the non-equilibrium compaction of clay rocks in sedimentary basins is formulated. The model generalizes those of earlier authors. The simplest assumptions are made concerning the rheology, and diagenesis is neglected. In this case, we show that the model reduces to a generalized consolidation equation, which for the classical Darcy flow is a non-linear diffusion equation for the porosity, with a free boundary. The model is non-dimensionalized, and it is shown that solutions depend on one significant dimensionless parameter λ, which is the ratio of the Darcy flow rate and the sedimentation rate. The model is solved numerically, and asymptotic descriptions of the solutions are given for the cases of large and small λ.

Key words: abnormal pore pressure, compaction, sedimentary basins.

1 INTRODUCTION

A fundamental understanding of the mechanical and physico-chemical properties of clay layers in the earth's crust has important applications in the areas of petrology, sedimentology, soil mechanics, oil field engineering and geophysical research. In this paper, we seek to improve the understanding of the geological processes which lead to the generation of abnormally high pressures in compacting clay layers. In addition, we seek to understand better the membrane properties of clays which may cause the formation of 'seals' (Hunt 1990) that can maintain these overpressures for geologically significant periods of times in the order of millions of years. The incorporation of well-characterized material properties into a compaction model will improve our ability to predict the mechanical behaviour and stability of deeply buried shale layers and thus, help us to anticipate the presence of overpressured strata under the stress conditions often found in North Sea oil fields. Our work addresses the needs of the oil industry which is constantly seeking better fundamental models for clay–shale behaviour that can be incorporated into large-scale oil reservoir simulators. In addition, improved sediment compaction models will be of interest to sedimentologists who are concerned with basin analysis techniques such as 'backstripping'.

The subject of this paper is the mathematical modelling of compacting shale layers. We consider a sediment system consisting of a porous solid phase whose interstitial volume is saturated with a liquid which we call the pore fluid. Due to the action of gravity and the density difference between the two phases, the solid phase compacts under its own weight by reducing its porosity, thus leading to the expulsion of the pore fluid out of the solid matrix. We adopt a continuum mechanics approach and write down equations for the conservation of mass and momentum. Assuming that the pore fluid motion is governed by Darcy's law, we derive a non-linear diffusion equation in terms of the porosity for the one-dimensional, non-equilibrium, gravity-driven compaction of sediments. We use a finite-difference technique to solve the non-linear equation for the case in which a sediment layer is forming over an impermeable, rigid basin floor due to the continuous deposition of solids at a constant rate. The equation is made dimensionless by appropriate scaling of the variables in order to make the solution independent of any system of units and to facilitate the interpretation of the results.

In order to simplify the task of developing the model, we have made a number of physically reasonable assumptions. First, we consider one-dimensional compaction instead of the more general cases in two or three dimensions. Despite its simplicity, one-dimensional compaction is applicable to many situations, for example, for the case in which the basin depth is small compared to its length and width. In addition, it is important to note that real world geophysical problems are very complicated and it is rare that enough information is known about the physical problem in order to prescribe enough boundary conditions to make the model mathematically well-posed. Thus, for purposes of trying to understand the gross effects of specific physical phenomena such as diagenesis for example, it is often wise to first consider a one-dimensional problem before investing additional effort in developing a two- or three-dimensional model. Second, we assume that Terzaghi's principle of effective stress

applies to clays over the range of stress conditions we are investigating. Third, we neglect the compressibilities of the individual phases and take the densities of the solid phase and the liquid phase to be constants.

We also make some further restrictions in our analysis which we will relax as the model undergoes future development. We initially take our sediment system to be isothermal and we omit the energy equation in our problem formulation. In addition, we assume that there are no chemical reactions in the system such as diagenetic transformations. Since reaction rates are temperature sensitive, diagenesis modelling and thermal effects will have to be included simultaneously. Two important input parameters in the model are the permeability, which depends on the porosity, and the constitutive law that describes the stress–strain relation of the clay. As a first approximation, we assume that the permeability follows a simple Cozeny–Karman law and that the constitutive relationship can be based on Athy's law. We want to emphasize that these are only temporary assumptions. In the future, our permeability model will be chosen based on carefully measured permeability data for montmorillonite. A more realistic constitutive law will be used that incorporates the irreversible, elastic–plastic behaviour of swelling.

In this paper, we first present a brief review of the compaction models currently discussed in the open literature. We then present a general multiphase flow model for compaction. This is then simplified to a non-dimensional model for isothermal compaction with no source terms, that is, no chemical reactions, along with the appropriate boundary conditions. A description of the method of numerical solution is also given. Results are presented for the specific case of 'normal compaction' in which a sediment layer forms as a result of sediment deposition at a constant rate.

2 LITERATURE REVIEW

The basic ideas about compaction and consolidation are discussed briefly in many textbooks on soil mechanics. We note that there is a sizeable body of knowledge concerning compaction modelling due to the efforts of the oil industry, but since it is often proprietary and unavailable to the general academic community, we are unable to discuss it in this section. This brief review serves as an introductory background to the subject matter.

Clay consolidation was modelled by Gibson (1958). This paper is a classic example of *linear* compaction theory in which it is assumed that the clay permeability and compressibility are constant, a drastic assumption which is sufficiently accurate for modelling thin clay layers often encountered in civil engineering problems. However, this is certainly invalid for clay layers deeply embedded in the earth's crust. Gibson examined several problems in which a sediment layer grows in time by the continuous deposition of solids at some prescribed rate. Two cases are examined, first, the case where the basin depth grows with the square root of time, and second, the case where the depth grows linearly with time. In addition, two different boundary conditions were considered for the basin floor; it being either permeable or impermeable. The major conclusion from this work was that excess pore pressures could occur in a continuously growing sediment layer. One useful feature of this work is that the solutions to the governing equations are given in closed form as opposed to numerical solutions and can thus be used directly in other contexts.

The next major works examining sedimentary clay layers were by Bredehoeft & Hanshaw (1968) and Hanshaw & Bredehoeft (1968). Both of these papers were based on linear consolidation theory and essentially used the solutions from Gibson's paper. The major innovation involved the modelling of diagenesis as a layer of source rock which produces pore water. It was concluded that sources of fluid could lead to overpressuring under certain circumstances in which the sediments surrounding the source layer were sufficiently low in permeability.

The next major step in the development of compaction models was by Smith (1971) who derived a non-linear compaction model that took into account permeability changes with changing porosity by assuming the validity of the Cozeny–Karman relationship. The stress–strain behaviour of the clay was taken to follow Athy's law. The resulting non-linear equations were solved numerically using a finite-difference technique. The problem considered was that of a sediment layer growing linearly in time over an impermeable basin floor.

The next major step involved the coupling of heat transfer with compaction as was done by Sharp & Domenico (1976) and Sharp (1976). Even though the results generally appear plausible, it should be noted that there is a conceptual mistake in one of the governing equations in the work of Sharp (1976) which was eventually corrected in a subsequent paper, Sharp (1983).

A different problem was examined by Bishop (1979) who considered the case of a thin shale layer being buried by a highly permeable layer of overburden. The compaction of the shale layer was modelled by linear compaction theory using the model from Gibson (1958). An interesting feature of the solutions was the prediction of a density inversion near the overburden–shale layer interface.

The work by Keith & Rimstidt (1985) was similar to the earlier work by Smith (1971). A non-linear compaction model was used and fluid generating source rocks were incorporated to mimic the effects of smectite–illite transformation. Unfortunately, the numerical method used to solve the non-linear equations was not robust and considerable difficulties were encountered unless the parameters of the permeability model were restricted to a specific range of values. Since the permeability model was chosen to guarantee convergence of the numerical scheme, the usefulness of the results are difficult to assess even though they appear to be qualitatively correct. As in many of the earlier models, an Athy-type constitutive law was used.

The first published attempt at a two-dimensional model was by Bethke (1985) in which material properties were taken to be temperature dependent. There are some serious objections to this model. The solid phase is restricted to vertical motion only and there is no liquid phase continuity equation. Despite this, two-dimensional Darcy flow is allowed and a two-dimensional heat transfer is provided for. The model uses Athy's law for the material behaviour and an empirical model for the permeability. In all, this model is

based on a wide range of assumptions which are not internally self-consistent. Thus, the validity of the results are open to severe criticism despite the fact that the underlying motivation for the work was sound and clearly stated. There is a comment on this work by Palciauskas (1988) and a reply by Bethke (1988). Finally, Bethke & Corbet (1988) extended the linear compaction model by allowing the permeability and the compressibility to be dependent on the porosity. These extensions represent partial linearizations of the non-linear model by Smith (1971). Since the extensions are not derived systematically from the non-linear model, it is difficult to interpret what physical assumptions they are actually based on.

All of these one-dimensional models currently in the literature suffer from two major deficiencies, first, the lack of accurate permeability data on which to select a proper permeability model, and second, the lack of good experimental data for the stress–strain behaviour of clay on which to formulate an adequate constitutive model. In addition, none of these models is put in dimensionless form and as a result, it is difficult to compare results from among the various models. Finally, diagenesis has not been treated properly except by the introduction of fluid-producing source rocks. Thus, it is clear from this brief introduction that there is a need for additional work in compaction modelling even for the simple one-dimensional cases.

3 THE BASIC MODEL FOR CONSOLIDATION AND DIAGENESIS

In a series of reports produced between 1975 and 1979, the Mathematics Clinic at Claremont College undertook work sponsored by Chevron Oil Company aimed at understanding the formation of high pore pressures in sedimentary basins. The most important parts of this work may be elucidated from the earliest and latest reports (Biedenweg *et al.* 1975; Lambert *et al.* 1979), and the model enunciated below is mostly based on their formulation. The Claremont modelling effort ended inconclusively, since, although a comprehensive model was proposed, it was not even non-dimensionalized, and consequently, attempts at numerical computations were hindered. Nevertheless, the Claremont reports provide a significant conceptual advance over much of the published literature. We now propose our version of their model.

3.1 Mass conservation

We consider a matrix which, in its eventual generality, will consist of four interdispersed media: coarse particles (e.g. quartz), two clay minerals, (hydrated) montmorillonite and (dehydrated) illite, and free pore water. Depending ultimately on the submodel which is used to describe diagenesis, a more complicated set of constituents may be necessary. In fact, the Chevron model allows for any number of intermediate (partially hydrated) clay minerals.

We denote the volume fractions of the respective media (coarse, montmorillonite, illite, water) by $\phi_c, \phi_m, \phi_i, \phi_l$, so that

$$\phi_c + \phi_m + \phi_i + \phi_l = 1, \tag{3.1}$$

and we suppose that the solids all move with the same averaged velocity $\mathbf{u}^s$, while the pore water has velocity $\mathbf{u}^l$. In a more complicated model in which mineral precipitation and pressure solution is included, the various solid velocities might be different.

We pose conservation of mass equations for the four phases in the form

$$\begin{aligned}
&\frac{\partial}{\partial t}(\rho_c\phi_c) + \nabla\cdot[\rho_c\phi_c\mathbf{u}^s] = 0,\\
&\frac{\partial}{\partial t}(\rho_m\phi_m) + \nabla\cdot[\rho_m\phi_m\mathbf{u}^s] = -r_m,\\
&\frac{\partial}{\partial t}(\rho_i\phi_i) + \nabla\cdot[\rho_i\phi_i\mathbf{u}^s] = r_i,\\
&\frac{\partial}{\partial t}(\rho_l\phi_l) + \nabla\cdot[\rho_l\phi_l\mathbf{u}^l] = r_w,
\end{aligned} \tag{3.2}$$

in which we suppose quartz particles are inert, but that clay particles can be transformed by dehydration processes which release bound water. The rate at which montmorillonite is transformed is denoted by r_m, and this is balanced by a production of illite at rate r_i, and of free pore water at rate r_w. In particular, total conservation of mass implies

$$r_m = r_i + r_w. \tag{3.3}$$

3.2 Diagenesis

In this first treatment, we will ultimately neglect diagenesis, but for completeness (or reference) we discuss here one way in which this process might be modelled. If we think of the dehydration process as a one-step reaction, we can represent it schematically as

$$\underset{\text{montmorillonite}}{[\text{clay}]}\cdot h[H_2O] \xrightarrow{k} \underset{\text{illite}}{[\text{clay}]} + \underset{\text{free water}}{h[H_2O]}\ , \tag{3.4}$$

in which we suppose montmorillonite is 'clay' with h moles of bound water per mole of clay. Let $[M], [I], [W]$ denote the molar concentrations (i.e. mol cm^{-3}) of montmorillonite, illite and free water, respectively; then the law of mass action applied to the first-order 'reaction' (3.4) suggests (for a homogeneous reaction)

$$\begin{aligned}
&[\dot{M}] = -k[M],\\
&[\dot{I}] = k[M],\\
&[\dot{W}] = hk[M].
\end{aligned} \tag{3.5}$$

The molar concentrations are related to the volume fractions by

$$\begin{aligned}
&[M] = \rho_m\phi_m/M_m,\\
&[I] = \rho_i\phi_i/M_i,\\
&[W] = \rho_w\phi_w/M_w,
\end{aligned} \tag{3.6}$$

where M_m, M_i, M_w are the respective molecular weights. It follows from (3.2) that the prescription of the rates there is given by

$$\begin{aligned}
&r_m = k\rho_m\phi_m,\\
&r_i = (M_i/M_w)r_m,\\
&r_w = (hM_w/M_m)r_m,
\end{aligned} \tag{3.7}$$

and (3.3) is automatically satisfied, since from (3.4) it is

clear that

$$M_m = M_i + hM_w. \tag{3.8}$$

3.3 Temperature

The simplest model would have r_m (or k) prescribed as a function of temperature and pressure, corresponding to an activated process. If r depends on temperature, then it is necessary to solve an energy equation. We suppose each phase has the same temperature T. A suitable model is then

$$\frac{\partial}{\partial t}\{[\rho_c c_c \phi_c + \rho_m c_m \phi_m + \rho_i c_i \phi_i + \rho_l c_l \phi_l]T\}$$
$$+ \nabla \cdot \{[(\rho_c c_c \phi_c + \rho_m c_m \phi_m + \rho_i c_i \phi_i)\mathbf{u}^s + \rho_l c_l \phi_l \mathbf{u}^l]T\}$$
$$= \nabla \cdot [k_{th} \nabla T] - r_m \Delta H, \tag{3.9}$$

where c_j are the various specific heats, k_{th} is a suitably defined average thermal conductivity, for example

$$k_{th} = \phi_c k_c + \phi_m k_m + \phi_i k_i + \phi_l k_l, \tag{3.10}$$

with obvious notation, and ΔH is the heat of (diagenetic) reaction. A simpler form of this equation would be sufficient for most purposes, and follows from taking the specific heats per unit volume as equal, thus $\rho_j c_j = \rho c$, and

$$\frac{\partial}{\partial t}(\rho c T) + \nabla \cdot [\rho c\{(1-\phi_l)\mathbf{u}^s + \phi_l \mathbf{u}^l\}T]$$
$$= \nabla \cdot [k_{th} \nabla T] - r_m \Delta H. \tag{3.11}$$

3.4 Stresses

Some divergence between different approaches to multi-phase flow modelling arises in consideration of the pressures, or more generally the stresses exerted on each constituent. First, we will assume that the average stress in each solid constituent is the same. Denote the *phase*-averaged stresses in solid and liquid to be σ^s and σ^l respectively (i.e., take a small volume V of the medium which, however, contains a large number of solid grains, and put $\sigma^s = (1/V_s)\int_{V_s} \hat{\sigma}^s \, dV$, where V_s is the part of V occupied, by solids, $\hat{\sigma}^s$ is the point value of the solid stress tensor). Averaged equations of two-phase flow (Drew 1983; Drew & Wood 1985) deal with these phasic averages. On the other hand, soil or rock mechanics typically seems to deal with the more obviously measurable *volume*-averaged stresses $\bar{\sigma}^s = (1/V)\int_{V_s} \hat{\sigma}^s \, dV$, etc. The relation between these is, for a *locally homogeneous medium* (i.e. one where surface averaging is equivalent to volume averaging),

$$\bar{\sigma}^s = \phi_s \sigma^s, \qquad \bar{\sigma}^l = \phi_l \sigma^l, \tag{3.12}$$

where $\phi_s = 1 - \phi_l$, ϕ_l are the relevant volume fractions. This distinction is not commonly made.

The total (bulk) applied stress is given as

$$\sigma = \phi_s \sigma^s + \phi_l \sigma^l = \bar{\sigma}^s + \bar{\sigma}^l, \tag{3.13}$$

and Terzaghi's effective stress σ_e is then defined by (Terzaghi 1936)

$$\sigma_e = \sigma - \bar{\sigma}^l; \tag{3.14}$$

we see that $\sigma_e = \bar{\sigma}^s$, and is the stress supported by the rock matrix. It is a principle of soil mechanics, to which we will also adhere, that deformation of the rock matrix is determined solely by the *effective* stresses. The negative traces (adopting the fluid mechanical sign convention) of the stress tensors define the *phase*-averaged pore pressure p^l, the volume-averaged $\bar{p}^l = \phi_l p^l$, and in particular Terzaghi's effective pressure p_e is defined by

$$p_e = P - \bar{p}^l = P - \phi_l p^l, \tag{3.15}$$

where P is the bulk pressure. It is important to note that the usual relation involves $\bar{p}^l$ and not p^l.

The issue of the proper definition of effective stress has been studied by Skempton (1960). In common with other authors, he makes no distinction between different definitions of pore pressure. However, he does suggest that the correct general definition of effective pressure is

$$p_e = P - a p^l, \tag{3.16}$$

where $(1-a)$ is essentially the grain to grain contact surface area per unit (grain) area. Thus for soils where contact area tends to zero, $a \to 1$ and we regain Terzaghi's result. On the other hand, assumption of local homogeneity in the granular medium would imply $1 - a = \phi_s$ and hence (3.15). We therefore see that it is possible to reconcile the solid mechanics assumptions with classical averaging methods by virtue of the non-uniformity of contact surface area. Skempton suggests that for rocks where significant contact occurs, $1-a$ is unlikely to be small. Indeed, we might expect (3.15) to be more accurate as ϕ_l becomes small.

3.5 Darcy's law

The distinction between phase and volume-averaged pressures makes its appearance in the derivation of Darcy's law (Fowler 1990). We assume that the liquid sustains no macroscopic stress, so that

$$\sigma^l = -p^l \delta; \tag{3.17}$$

Darcy's law then takes the form

$$\phi_l(\mathbf{u}^l - \mathbf{u}^s) = -\frac{k}{\mu}(\nabla p^l + \rho_l g \mathbf{j}), \tag{3.18}$$

where $\mathbf{j}$ is a unit vector pointing vertically upwards, k is the matrix permeability, and μ is the liquid viscosity.

3.6 Force balance

For a slow flow, the total momentum equation can be written

$$\nabla \cdot \sigma + \rho \mathbf{g} = 0, \tag{3.19}$$

where the density is

$$\rho = \rho_s \phi_s + \rho_l \phi_l. \tag{3.20}$$

3.7 Rheological laws

We now come to the complicated question of prescribing an appropriate constitutive relation for the rock rheology. The principle of effective stress implies (and we assume) that $\mathbf{u}^s$ and its derivatives should depend on the effective stress σ_e. Below we flag some relevant models which have been discussed.

3.7.1 Athy model

Based on the experimental observations in sedimentary basins by Athy (1930), Rubey & Hubbert (1959) proposed a direct relationship between the porosity ϕ_1 and the effective pressure p_e. In its simplest form, this relation is of the form

$$\phi = \phi(p_e), \text{ for example } = \phi_0 \exp[-bp_e]. \tag{3.21}$$

In fact, the observations are such that $\rho = \rho(Z)$, where Z is depth, and it is through the dependence of p_e on ρ that relations such as (3.21) can be inferred (e.g. Smith 1971). Thus while the porosity–depth relation for normally pressured rocks seems robust, the inference of a relation between ϕ and p_e is merely a convenience.

3.7.2 One-dimensional theory

In order to place Athy's law in a proper context, we recall the results of isotropic and one-dimensional (oedometer) compression tests for soils (and rocks) (Burland 1990). As illustrated in Fig. 1, the behaviour of soils under increasing compression is not reversible. There is a 'transient' part of the curve for small p_e, and then as p_e is increased, the values of void ratio $e = \phi/(1-\phi)$ arrive at a curve called the normal consolidation line. It seems that we should interpret (3.21) as representing the normal consolidation line (NCL) for sedimentary rocks. So long as p_e increases, e decreases along the NCL, but if p_e is decreased, then e moves back (more or less reversibly) along a shallower curve. This behaviour is analogous to the elastic–plastic behaviour of metals, for example. In order to model it, we would define p_e^* to be the maximum value of p_e in the time-history of compaction. If $p_e < p_e^*$, the soil is said to be *over-consolidated.*

The usual functional form for the relation between e and p_e on the NCL is

$$e = e_0 - C_c \ln(p_e/p_0), \tag{3.22}$$

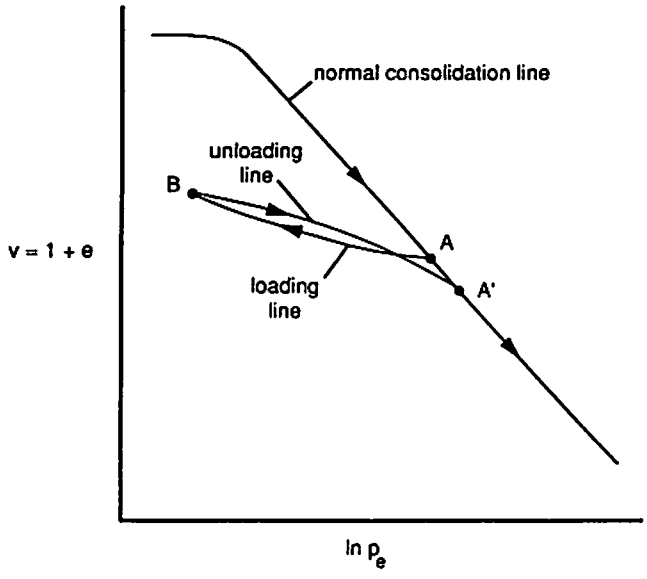

Figure 1. Consolidation of soils.

where C_c is termed the compression index. Since

$$e = \phi/(1-\phi), \tag{3.23}$$

we see that (3.22) bears little resemblance to (3.21).

In order to model the elastic–plastic behaviour, we suppose that

$$e = e_0' - C_s \ln(p_e/p_0) \tag{3.24}$$

gives the elastic response if $p_e < p^*$, where C_s is called the swelling index. Here e_0' is related to (3.22) by

$$e_0' - C_s \ln(p^*/p_0) = e_0 - C_c \ln(p_e^*/p_0), \tag{3.25}$$

i.e.

$$e_0' = e_0 - (C_c - C_s) \ln(p_e^*/p_0). \tag{3.26}$$

We thus have

$$e = e_0 - (C_c - C_s) \ln(p_e^*/p_0) - C_s \ln(p_e/p_0), \tag{3.27}$$

if $p_e < p^*$, while if $p_e = p^*$, then on the NCL,

$$e = e_0 - C_c \ln(p_e/p_0). \tag{3.28}$$

The definition of p_e^* is simply written, if $d/dt_s \equiv \partial/\partial t + \mathbf{u}^s \cdot \nabla$ denotes a time derivative following the solid matrix. Evidently

$$\begin{aligned} \frac{dp_e^*}{dt_s} &= H(p_e - p_e^*)\frac{dp_e}{dt_s} H(dp_e/dt_s) \\ &= H(p_e - p_e^*)(dp_e/dt_s)_+, \end{aligned} \tag{3.29}$$

and ϕ is determined from (3.27) or (3.28).

3.8 Critical state theory

The question now arises as to how the compressibility diagram extends to two or three dimensions to include the effects of other stress components. When the stress field has two independent components (as in a triaxial test) this leads to the idea of a critical state surface.

First, the stress tensor is commonly taken with the opposite sign to the fluid mechanical (and our) convention: $\boldsymbol{\sigma}^R = -\boldsymbol{\sigma}$, where $\boldsymbol{\sigma}^R$ is the rock-defined stress tensor. The 'rock' effective stress is then

$$\boldsymbol{\sigma}' = \boldsymbol{\sigma}^R - \bar{p}^1 \boldsymbol{\delta}. \tag{3.30}$$

Suppose that $\boldsymbol{\sigma}'$ has principal stresses $\sigma_1', \sigma_2', \sigma_3'$ with $\sigma_2' = \sigma_3'$, and $\sigma_1' > \sigma_3'$. Thus σ_1' is the maximum compressive stress. Then the mean effective stress p' and deviatoric stress q' are defined by

$$\begin{aligned} p' &= \tfrac{1}{3}(\sigma_1' + 2\sigma_3'), \\ q' &= \sigma_1' - \sigma_3', \end{aligned} \tag{3.31}$$

where $p'(=p_e)$, q' are the commonly used symbols in soil mechanics. Many experimental results now show that a *critical state surface* can be defined as shown in Fig. 2. It consists of three surfaces: the Roscoe surface, the Hvorslev surface, and a tension failure surface. The join of the Hvorslev and Roscoe surfaces is called the *critical state line.*

The critical state surface is the continuation when $q' \neq 0$ of the normal consolidation line. Below the yield surface, behaviour is (more or less) elastic, while at the yield surface, plastic (irrecoverable) deformation takes place. Thus the

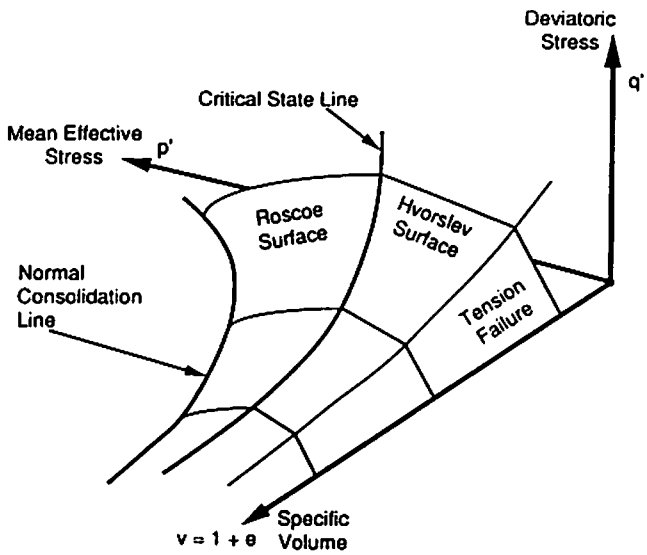

Figure 2. The critical state surface.

region above the critical state surface is inaccessible, at least to the elastic–plastic flow régime.

Excluding the tensional failure surface, the critical state surface can be represented in terms of five parameters: M, h, Γ, λ, N. Specifically (with $v = 1 + e$, the specific volume):

$$\begin{aligned} &\text{Hvorslev}: q' = (M-h)\exp[(\Gamma - v)/\lambda] + hp';\\ &\text{Roscoe}: v = N + (\Gamma - N)q'/Mp' - \lambda \ln p';\\ &\text{CSL}: q' = Mp', \quad v = \Gamma - \lambda \ln p';\\ &\text{NCL}: v = N - \lambda \ln p'. \end{aligned} \tag{3.32}$$

[Notice that the notation is different to that used earlier; this is that of Atkinson & Bransby (1978).] The yield surface described by equation (3.32) is the original Cam-clay model described by Schofield & Wroth (1968). More modern extensions, known as cap models, are described by Chen & Mizuno (1990).

Notice also that 'plasticity' on the critical state surface does not mean creep (necessarily): a given stress still leads to a finite strain. However, it is in addition likely that mechanisms such as pressure solution and microfracturing will lead to permanent creep, and this is consistent with experiments, where it is known as secondary consolidation [ordinary consolidation (Schiffman, Pane & Gibson 1984) being a time-dependent process resulting from transient adjustment of pore water pressure].

3.9 Poroelasticity theory

Having identified the region below the critical state surface (CSS) as one of essentially recoverable elastic deformation, we must pose an appropriate elasticity theory. Such a theory was given by Biot (1941), whose concern was consolidation. He proposed an elastic constitutive relation between total stress σ and the strain tensor ϵ where $\epsilon_{ij} = \frac{1}{2}(\partial U_i/\partial x_j + \partial U_j/\partial x_i)$ and $\mathbf{U}$ is the strain field. This is

$$\sigma = 2G\epsilon + \left(\frac{2Gv}{1-2v}\nabla\cdot\mathbf{U} - \alpha p'\right)\delta; \tag{3.33}$$

this was *supplemented* by a constitutive relation for ϕ (or p'):

$$\phi - \phi_0 = \frac{1}{Q}p' + \alpha\nabla\cdot\mathbf{U}. \tag{3.34}$$

The relation (3.33) is equivalent to an ordinary elastic medium, with the pressure defined by

$$-\tfrac{1}{3}\sigma_{ii} = P = \alpha p' - \frac{2G(1-\nu)}{3(1-2\nu)}\nabla\cdot\mathbf{U}, \tag{3.35}$$

whence (3.34) is

$$\phi - \phi_0 = \frac{1}{Q}p' - \frac{3\alpha(1-2\nu)}{2G(1+\nu)}(P - \alpha p'). \tag{3.36}$$

For a saturated clay, Biot suggests $Q = \infty$, $\alpha = 1$, whence (3.36) is

$$\phi - \phi_0 = \frac{3(1-2\nu)}{2G(1+\nu)}p_e, \tag{3.37}$$

and (3.25) is

$$P - p' = p_e = -\frac{2G(1+\nu)}{3(1-2\nu)}\nabla\cdot\mathbf{U}. \tag{3.38}$$

Biot's is a linear theory, representing perturbations about a basic state $\phi = \phi_0$, $p_e = 0$. As such, (3.37) may be suggestively written

$$\delta\phi \approx -\delta p_e/K, \tag{3.39}$$

where K is some kind of elasticity modulus, which for larger perturbations should depend on p_e: thus we regain the swelling curves (3.24). [Specifically, $v = 1/(1-\phi) = v_0 - C_s \ln p_e$, thus $\delta\phi = -C_s(1-\phi)^2\delta p_e/p_e$, or $K = p_e/C_s(1-\phi)^2$.] Intuitively, in Biot's theory, the basic constitutive law for the rheology is *supplemented* by a *separate* constitutive relation for the effective pressure. This is in accordance with multiphase flow theory, where each extra pressure requires a separate constitutive relation.

In incorporating a differential relation such as (3.39) into a compaction theory, we must recognize that the solids may move substantially. Then the appropriate time derivative indicated for (3.39) is one following the solid, i.e.

$$\frac{d\phi}{dt_s} = -\frac{1}{K}\frac{dp_e}{dt_s}, \tag{3.40}$$

where $d/dt_s = \partial/\partial t + \mathbf{u}^s\cdot\nabla$. In simple compaction models involving loading only, the elasticity relation is irrelevant (it serves to determine the uncoupled horizontal stress). Similarly since $d/dt_s\,\nabla\cdot\mathbf{U} = \nabla\cdot\mathbf{u}^s$, (3.28) is

$$\frac{dp_e}{dt_s} = -K\nabla\cdot\mathbf{u}^s, \tag{3.41}$$

which is identical to (3.40) via mass conservation if ρ_s is constant.

4 A SIMPLIFIED MODEL

The basic Chevron (-type) model can be summarized as follows.

Mass conservation:

$$\begin{aligned}
&\frac{\partial}{\partial t}(\rho_c\phi_c) + \nabla\cdot(\rho_c\phi_c\mathbf{u}^s) = 0,\\
&\frac{\partial}{\partial t}(\rho_m\phi_m) + \nabla\cdot(\rho_m\phi_m\mathbf{u}^s) = -r_m,\\
&\frac{\partial}{\partial t}(\rho_i\phi_i) + \nabla\cdot(\rho_i\phi_i\mathbf{u}^s) = r_i,\\
&\frac{\partial}{\partial t}(\rho_l\phi_l) + \nabla\cdot(\rho_l\phi_l\mathbf{u}^l) = r_w.
\end{aligned} \tag{4.1}$$

Energy conservation:

$$\begin{aligned}
&\frac{\partial}{\partial t}(\rho cT) + \nabla\cdot\{\rho c[(1-\phi_l)\mathbf{u}^s + \phi_l\mathbf{u}^l]T\}\\
&\quad = \nabla\cdot(k\nabla T) - r_m\Delta H.
\end{aligned} \tag{4.2}$$

Darcy's law:

$$\phi_l(\mathbf{u}^l - \mathbf{u}^s) = -\frac{k}{\mu}(\nabla p^l + \rho_l g\mathbf{j}). \tag{4.3}$$

Force balance:

$$\nabla\cdot\boldsymbol{\sigma}_e - \nabla(\bar{p}^l) + \rho\mathbf{g} = 0. \tag{4.4}$$

Rheological constitutive relationships:
e.g. elastic:

$$\boldsymbol{\sigma}_e = 2G\boldsymbol{\epsilon} - (p_e + \tfrac{2}{3}G\nabla\cdot\mathbf{U})\boldsymbol{\delta}, \tag{4.5}$$

with a constitutive relation, for effective pressure, such as

$$\frac{dp_e}{dt_s} = -K\nabla\cdot\mathbf{u}^s, \tag{4.6}$$

[or equivalently $p_e = p_e(\phi)$]. To follow (4.5) with a material element, we have

$$\frac{d\boldsymbol{\sigma}_e}{dt_s} = 2G\dot{\boldsymbol{\epsilon}} - (\dot{p}_e + \tfrac{2}{3}G\nabla\cdot\mathbf{u}^s)\boldsymbol{\delta}. \tag{4.7}$$

In what follows, we will begin by adopting the simplest model which exhibits the phenomenon of non-linear compaction. Complications to this model will be added in later work. We restrict attention to a single solid species of density ρ_s. We put $\phi_l = \phi$, $\phi_s = 1-\phi$, and ignore the source terms due to diagenesis. Finally, we consider a one-dimensional model in a basin $b(t) < z < h(t)$, where h is the ocean floor, and b is the basement rock as depicted in Fig. 3. The governing equations are then (with $p^l = p$)

$$\begin{aligned}
&\frac{\partial\phi}{\partial t} + \frac{\partial}{\partial z}[\phi u^l] = 0,\\
&-\frac{\partial\phi}{\partial t} + \frac{\partial}{\partial z}[(1-\phi)u^s] = 0,\\
&\phi(u^l - u^s) = -\frac{k}{\mu}\left(\frac{\partial p}{\partial z} + \rho_l g\right);
\end{aligned} \tag{4.8}$$

the effective stress tensor is of the form

$$\boldsymbol{\sigma}_e = \mathrm{diag}\,(-\sigma_1', -\sigma_3', -\sigma_3'), \tag{4.9}$$

where the minus sign is introduced in keeping with rock mechanics usage. Thus

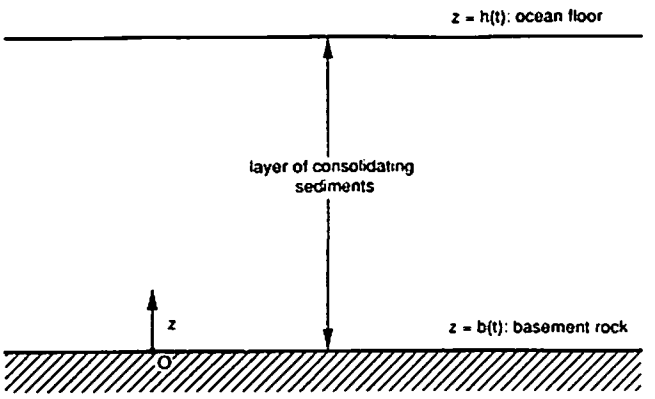

Figure 3. A schematic representation of the sedimentary basin undergoing one-dimensional consolidation. The coordinate z is chosen such that the ocean floor is located at $z = h(t)$ and the basin basement is at $z = b(t)$. Gravity acts in the negative z direction.

$$-\frac{\partial\sigma_3'}{\partial z} - \frac{\partial\bar{p}}{\partial z} - [\rho_s(1-\phi) + \rho_l\phi]g = 0, \tag{4.10}$$

(writing $\bar{p}^l = \bar{p}$), and if we assume an elastic law such as (4.7) with (4.6), then

$$-\dot{\sigma}_1' = -\left(\dot{p}_e + \frac{2}{3}G\frac{\partial u^s}{\partial z}\right), \tag{4.11}$$

where $\dot{}$ denotes $\partial/\partial t + u^s\,\partial/\partial z$, and

$$-\dot{\sigma}_3' = -\dot{p}_e + \frac{4}{3}G\frac{\partial u^s}{\partial z}, \tag{4.12}$$

$$\dot{p}_e = -K\frac{\partial u^s}{\partial z}. \tag{4.13}$$

Thus

$$\begin{aligned}
&\sigma_1' = \left(1 - \frac{2G}{3K}\right)p_e,\\
&\sigma_3' = \left(1 + \frac{4G}{3K}\right)p_e,
\end{aligned} \tag{4.14}$$

and from (4.13) and (4.8),

$$\dot{p}_e = -K\frac{\partial u^s}{\partial z} = -K\dot{\phi}, \tag{4.15}$$

whence we have an Athy-type law

$$p_e = p_e(\phi), \tag{4.16}$$

if $K = K(p_e, \phi)$.

The simple model is therefore

$$\begin{aligned}
&\frac{\partial\phi}{\partial t} + \frac{\partial}{\partial z}(\phi u^l) = 0,\\
&-\frac{\partial\phi}{\partial t} + \frac{\partial}{\partial z}[(1-\phi)u^s] = 0,\\
&\phi(u^l - u^s) = -\frac{k}{\mu}\left(\frac{\partial p}{\partial z} + \rho_l g\right),\\
&\frac{\partial}{\partial z}\left[-\left(1 + \frac{4G}{3K}\right)p_e - \bar{p}\right] - [\rho_s(1-\phi) + \rho_l\phi]g = 0,\\
&p_e = p_e(\phi),
\end{aligned} \tag{4.17}$$

for the variables ϕ, u^l, u^s, p, p^e, and where $\bar{p}$ needs to be constituted in terms of p, e.g. $\bar{p} = ap$, as discussed above.

4.1 Boundary conditions

We presume $b(t)$ is a known boundary, but $h(t)$ is unknown *a priori*. We require boundary conditions on u^l, u^s, p, p_e for the equations.

The natural boundary conditions are these—kinematic boundary conditions at $z = b$:

$$u^s = u^l = \dot{b}; \tag{4.18}$$

a kinematic condition at $z = h$:

$$\dot{h} = \dot{m}_s + u^s, \tag{4.19}$$

where $\dot{m}_s$ is the sedimentation rate at $z = h$. Also at $z = h$,

$$\phi = \phi_0 \text{ (equivalently, } p_e = 0), \qquad p = p_0, \tag{4.20}$$

where p_0 is the overburden (e.g. due to ocean depth). Equation (4.19) gives h, and then we have four conditions, for u^s, u^l, p_e and p, as required.

Adding $(4.17)_1$ and $(4.17)_2$, we find

$$\phi u^l + (1-\phi)u^s = \dot{b}; \tag{4.21}$$

therefore

$$\frac{\partial \phi}{\partial t} = \frac{\partial}{\partial z}[(1-\phi)u^s],$$
$$u^s = \dot{b} + \frac{k}{\mu}\left[\frac{\partial p}{\partial z} + \rho_l g\right], \tag{4.22}$$

and we see that ϕ satisfies a non-linear diffusion equation, provided p can be obtained as a function of ϕ. Thus we integrate $(4.17)_4$ to determine $p(\phi)$, using (4.20), and then solve (4.22) with

$$u_s = \dot{b} \text{ on } z = b, \qquad \phi = \phi_0 \text{ on } z = h, \tag{4.23}$$

and h is determined from (4.19).

The above model is essentially that of classical compaction theory, providing $\bar{p}$ in $(4.17)_4$ is set equal to p. In this paper, we follow Skempton (1960) in allowing $\bar{p} = ap$, $a \le 1$, but will assume that a is constant. In that case, we obtain a single non-linear diffusion equation for ϕ.

4.2 Non-dimensionalization

We define a length-scale d by writing

$$\left(1 + \frac{4G}{3K}\right)p_e = (\rho_s - \rho_l)g\, d(1-a)\bar{p}(\phi), \tag{4.24}$$

and requiring that $\bar{p} = O(1)$. In addition, we scale z with d, u^s with $\dot{m}_s$, time t with $d/\dot{m}_s$, pore pressure p with $(\rho_s - \rho_l)g\, d$, and permeability with k_0, i.e. we write

$$k = k_0 \bar{k}, \tag{4.25}$$

such that $\bar{k}(\phi) = O(1)$ (for example, when $\phi = \phi_0$). The dimensionless model is then

$$\frac{\partial \phi}{\partial t} = \frac{\partial}{\partial z}[(1-\phi)u^s],$$
$$u^s = \dot{b} + \lambda \bar{k}\left(\frac{\partial p}{\partial z} + r\right), \tag{4.26}$$

where

$$\lambda = \frac{k_0(\rho_s - \rho_l)g}{\mu \dot{m}_s}, \qquad r = \frac{\rho_l}{\rho_s - \rho_l}. \tag{4.27}$$

The pore pressure is determined by quadrature from $(4.16)_4$, which is

$$-(1-a)\frac{\partial}{\partial z}(\bar{p} + p) - (1 + r) + \phi = 0. \tag{4.28}$$

The variables in these equations are all dimensionless. The boundary conditions are

$$\frac{\partial p}{\partial z} + r = 0 \text{ at } z = b,$$
$$\phi = \phi_0, \qquad \dot{h} = \dot{b} + \dot{m} + \lambda \bar{k}\left(\frac{\partial p}{\partial z} + r\right) \text{ at } z = h. \tag{4.29}$$

Here, $\dot{m}$ is the *dimensionless* sedimentation rate: 1 if it is constant, or $O(1)$ if time-varying.

4.3 A non-linear diffusion equation

We substitute for $\partial p/\partial z$ from (4.28) into (4.26), where

$$\partial p/\partial z + r = -\partial \bar{p}/\partial z - \left[\frac{1 + ar - \phi}{1-a}\right], \tag{4.30}$$

and the equation is simply

$$\frac{\partial \phi}{\partial t} = -\dot{b}\frac{\partial \phi}{\partial z} + \lambda \frac{\partial}{\partial z}\left\{(1-\phi)\bar{k}\left[-\bar{p}'(\phi)\frac{\partial \phi}{\partial z} - \left(\frac{1 + ar - \phi}{1-a}\right)\right]\right\}, \tag{4.31}$$

a non-linear diffusion equation for ϕ, with boundary conditions

$$-\bar{p}'(\phi)\frac{\partial \phi}{\partial z} - \left(\frac{1 + ar - \phi}{1-a}\right) = 0 \quad \text{on } z = b,$$
$$\phi = \phi_0, \qquad \dot{h} - \dot{b} = \dot{m} + \lambda \bar{k}\left[-\bar{p}'(\phi)\frac{\partial \phi}{\partial z} - \left(\frac{1 + ar - \phi}{1-a}\right)\right]$$
$$\text{on } z = h. \tag{4.32}$$

By taking a moving frame of reference, we can clearly take $\dot{b} = 0$. Since $\bar{p}'(\phi) < 0$, (4.31) and (4.32) give a free boundary problem for ϕ, depending essentially only on the parameter λ.

In the following section, we will address the solution of *this* problem numerically and analytically. It is useful to do this, to compare solutions with previous work.To get an estimate for λ, we use the values, taken from observations, of $d \sim 4$ km, $k \sim 10^{-19}\,\text{m}^2$, $\Delta\rho \sim 1.6 \times 10^3\,\text{kg m}^{-3}$, $g \sim 10\,\text{m s}^{-2}$, $\mu \sim 2 \times 10^{-3}\,\text{N s m}^{-2}$, $\dot{m}_s \sim 150\,\text{m Ma}^{-1}$ $(=0.5 \times 10^{-11}\,\text{m s}^{-1})$; then $\lambda \approx 10$. Values of λ of $O(1)$ are therefore

of interest, with values of $\lambda \gg 1$ (slow sedimentation) or $\lambda \ll 1$ (fast sedimentation) also being relevant.

5 RESULTS AND ANALYSIS

For simplicity, and for comparison to previous work, we adopt here the classical model, which is given by (4.31) and (4.32), with $\dot{b} = 0$ and we take the specific contact area as $a = 0$ (this makes little difference to the solutions). Based on the work of Smith (1971), we use the following constitutive functions:

$$\bar{p} = \ln(\phi_0/\phi) - (\phi_0 - \phi),$$
$$\bar{k} = (\phi/\phi_0)^8, \qquad (5.1)$$
$$\dot{m} = 1.$$

We have solved the equations numerically for various values of λ. We use a fully implicit central difference method on a normalized grid parametrized by $Z = z/h(t)$. In the following figures, we show the evolution of porosity ϕ for times for which $h = O(10)$. Note that $h = 10$ corresponds to a depth of about 30 km, if $d = 3$ km.

(i) $\lambda \gg 1$

Fig. 4 shows the solution of ϕ as a function of Z for $t \leq 20$. On a time-scale $t = O(10)$, we see that for $Z = O(1)$, $\phi \sim \phi(Z)$. The same data is shown as a function of Z in Fig. 5. Here we can see that for $t > 2$ and $h - z \sim 1$, $\phi \sim \phi(h - z)$; this behaviour is further analysed below. Fig. 6 shows h versus t. For $t > 1$, it is very close to linear. Fig. 7 shows the pore pressure compared to hydrostatic and overburden at $t = 2$, when $h \approx 1.4$.

(ii) $\lambda = O(1)$

Figs 8 and 9 show the evolution of ϕ as a function of Z and z respectively for $\lambda = 1$. For $t \gg 1$, $Z \sim 1$, $\phi \sim \phi(Z)$,

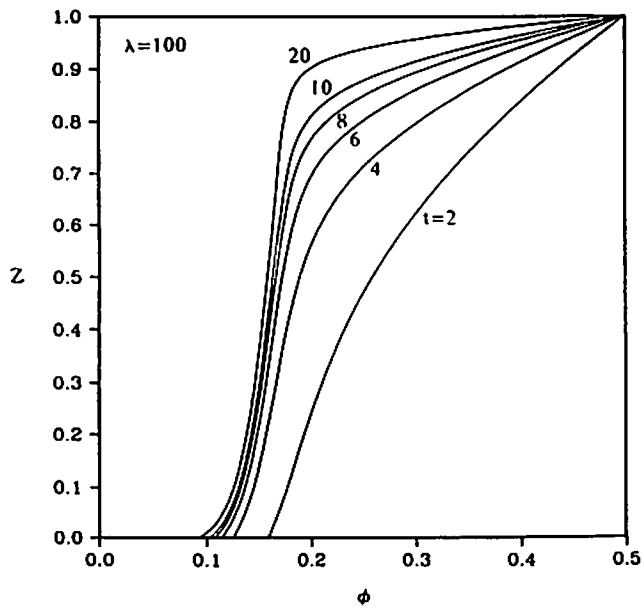

Figure 4. Porosity versus normalized depths at various times, $\lambda = 100$.

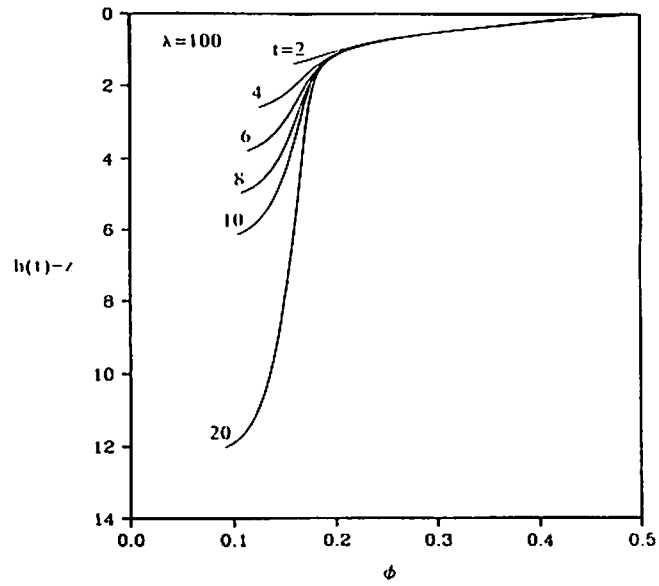

Figure 5. Porosity versus depth at various times, $\lambda = 100$.

while for $t \gg 1$, $h - z \sim 1$, $\phi \sim \phi(h - z)$. This is much as before, the only difference being that ϕ is smaller in the far field for higher λ. Again h is approximately linear for $t > 1$, with $h/t \approx 0.75$. Fig. 10 shows pore pressure as a function of Z at $t = 5$, together with overburden and hydrostatic values.

(iii) $\lambda \ll 1$

The solution is dramatically different when λ is small. Fig. 11 shows ϕ for various times as a function of z. Evidently, $\phi \approx \phi_0$ for $z \sim O(1)$, with a thin boundary layer of thickness $\sim 0.05h$ near $z = 0$ (see Fig. 12). It is also clear from Fig. 11 that $\dot{h} \approx 1$ in this limit. Finally, Fig. 13 shows the pore pressure profile at $t = 5$.

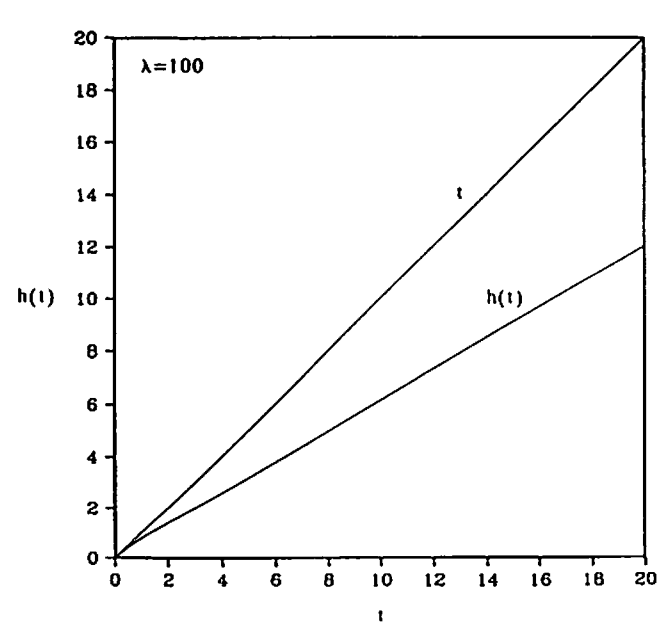

Figure 6. Basin thickness as a function of time, $\lambda = 100$.

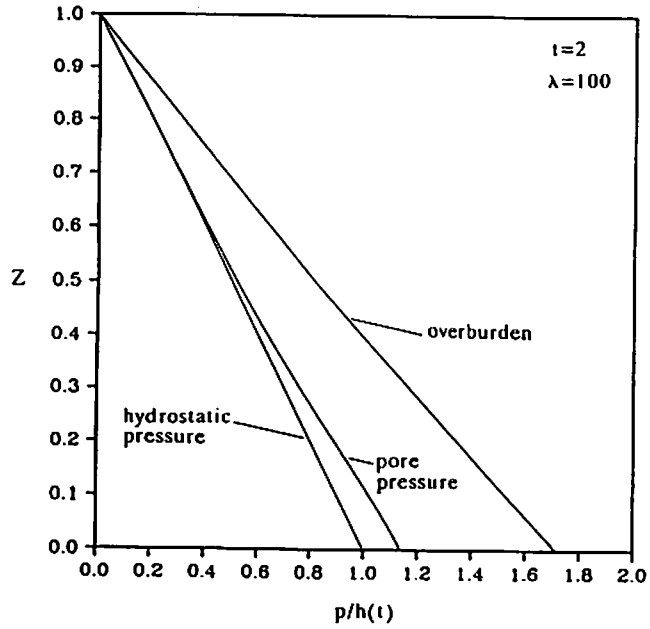

Figure 7. Hydrostatic, pore and overburden pressures at $t = 2$, $\lambda = 100$.

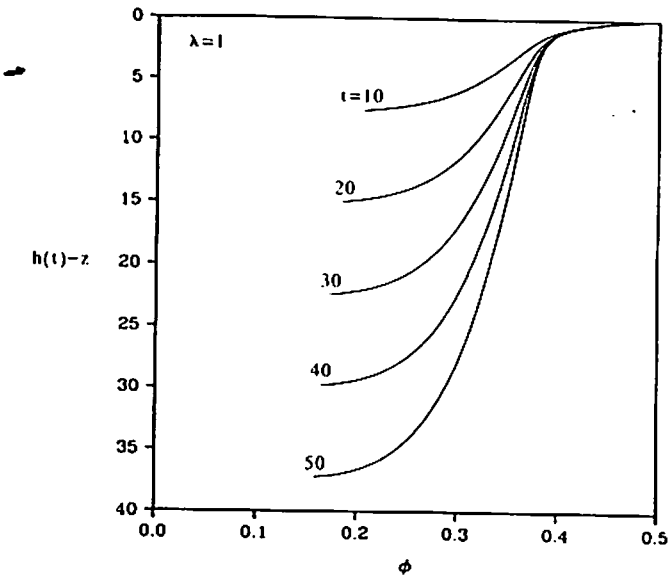

Figure 9. Porosity versus depth at various times, $\lambda = 1$.

5.1 Asymptotics

There are two distinct types of behaviour exhibited by these solutions, namely for $\lambda > 1$ and $\lambda \ll 1$, and we can give an approximate description of each of these. The analysis is based partly on the size of λ, but also to some extent on the largeness of the exponent for $\bar{k}$, i.e. $\bar{k} = (\phi/\phi_0)^m$, $m = 8 \gg 1$. First we write the model (4.31) and (4.32) with $a = 0$, $b = 0$, and incorporating (5.1), we find

$$\phi_t = \lambda \frac{\partial}{\partial z}\left\{\bar{k}(1-\phi)^2\left[\frac{1}{\phi}\frac{\partial \phi}{\partial z} - 1\right]\right\}, \tag{5.2}$$

with

on $z = 0$: $\phi_z - \phi = 0$;

$$\text{on } z = h\text{:}\quad \dot{h} = 1 + \lambda\bar{k}(1-\phi)\left(\frac{1}{\phi}\frac{\partial \phi}{\partial z} - 1\right), \tag{5.3}$$

$$\phi = \phi_0,$$

and where

$$\bar{k} = (\phi/\phi_0)^m, \qquad m = 8. \tag{5.4}$$

5.1.1 $\lambda > 1$

The numerical results suggest that for $z \sim t \gg 1$, we have

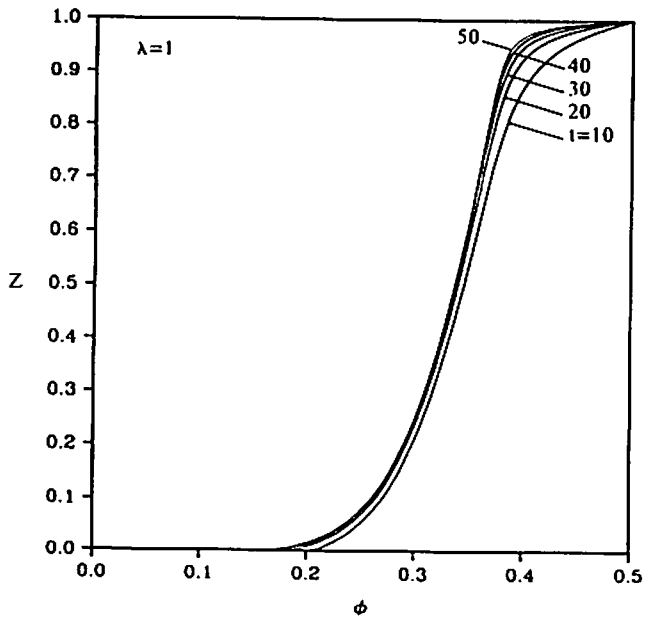

Figure 8. Porosity versus scaled height at various times, $\lambda = 1$.

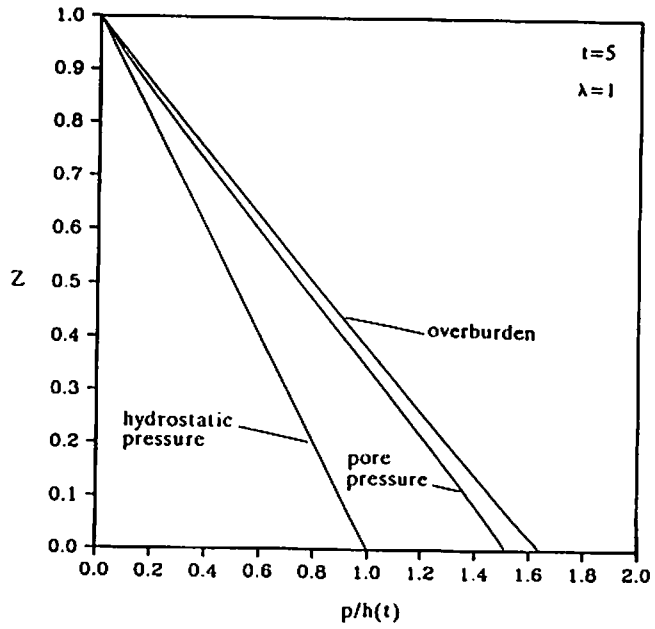

Figure 10. Hydrostatic, pore and overburden pressures at $t = 5$, $\lambda = 1$.

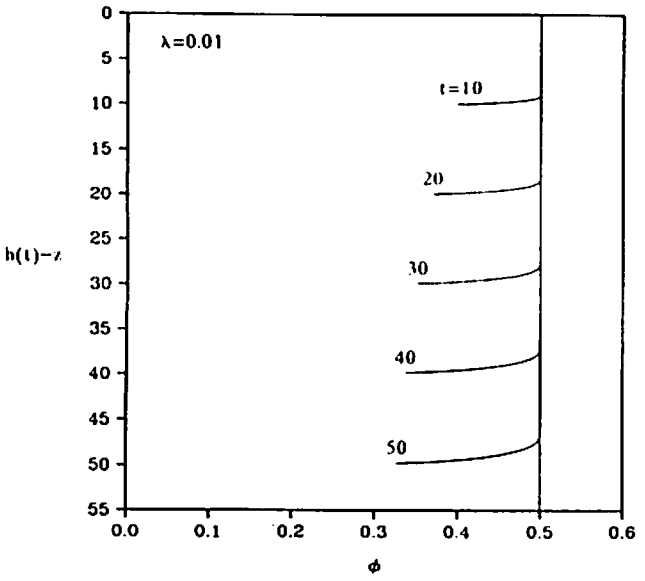

Figure 11. Porosity versus depth at various times, $\lambda = 0.01$.

$\phi \sim \phi(z/t)$. Therefore, define

$$\xi = z/t, \tag{5.5}$$

$$t\phi_t - \xi\phi_\xi = \lambda \frac{\partial}{\partial \xi}\left\{\bar{k}(1-\phi)^2\left[\frac{1}{t\phi}\frac{\partial \phi}{\partial \xi} - 1\right]\right\}. \tag{5.6}$$

At large times, we neglect the diffusive term and can expect an approximate steady state (note that the largeness of λ is likely to be offset by the smallness of $\bar{k}$), thus

$$\xi\phi_\xi \approx \lambda \frac{\partial}{\partial \xi}[\bar{k}(1-\phi)^2], \tag{5.7}$$

with implicit solution

$$\xi \approx \lambda \frac{d}{d\phi}[(1-\phi)^2(\phi/\phi_0)^m]. \tag{5.8}$$

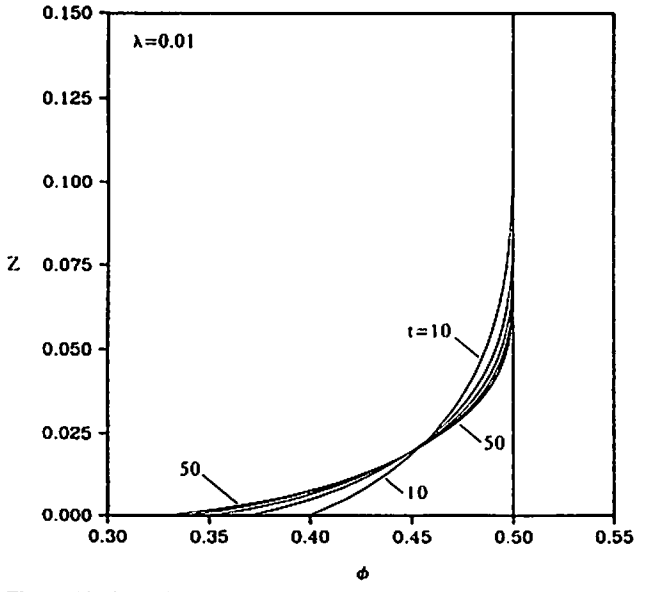

Figure 12. Porosity versus scaled height above basement at various times, $\lambda = 0{\cdot}01$.

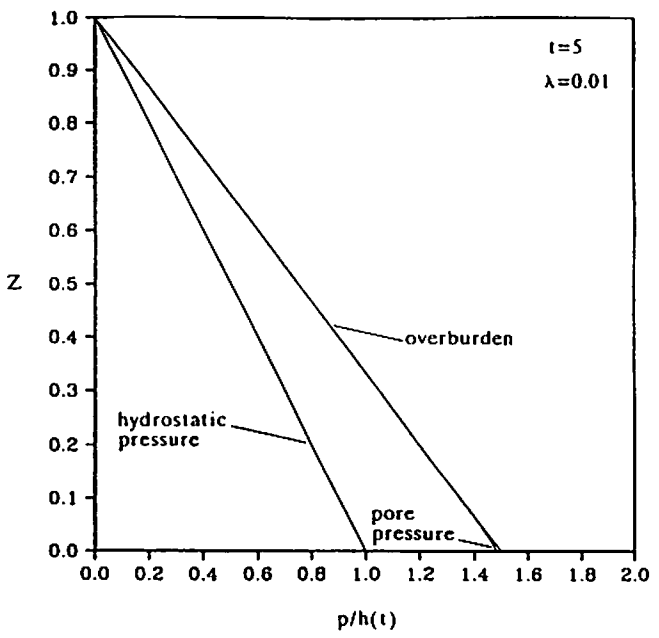

Figure 13. Hydrostatic, pore and overburden pressures at $t = 2$, $\lambda = 0.01$.

An approximate representation of (5.8) is obtained by expanding for large m, whence we find

$$\phi/\phi_0 \approx (\phi_0 \xi/m\lambda)^{1/(m-1)}. \tag{5.9}$$

It can be seen that this is consistent with Fig. 8, for example. The loss of the diffusion term means that we cannot satisfy boundary conditions at $z = 0$ or $z = h$. We will only consider that at $z = h$, which is the more interesting of the two.

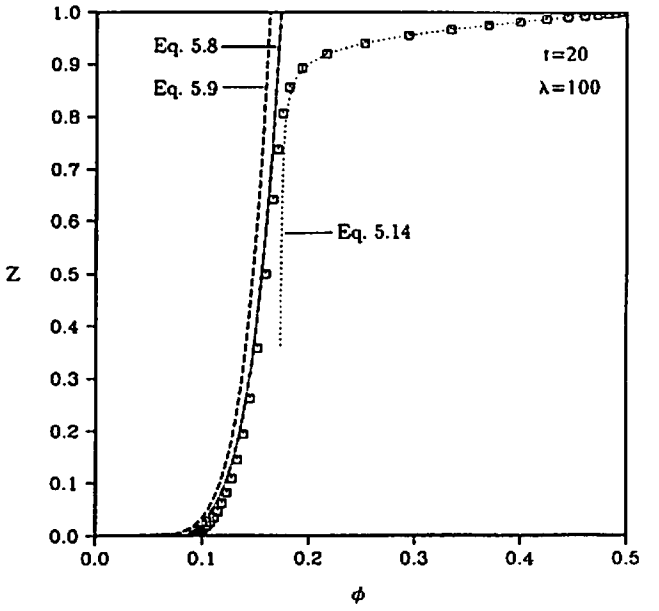

Figure 14. A comparison of the numerically calculated porosity profile $t = 20$ and $\lambda = 100$ to the asymptotic solutions for $\lambda \gg 1$. The numerical solution is shown by the squares. The inner solution (5.14) is shown by the dotted line and the matched outer solution, (5.8), is shown by the dashed–dotted line. The explicit approximation to the outer solution, that is (5.9), is shown by the dashed line.

Near $z = h$, Fig. 9 suggests $\phi \approx \phi(h - z)$, and also the solution has $h \sim t$. Therefore we put

$$\eta = ct - z, \qquad h \approx ct, \tag{5.10}$$

and seek a steady solution in this moving frame. We have

$$c\phi' = -\lambda\left\{\bar{k}(1-\phi)^2\left[-\frac{1}{\phi}\phi' - 1\right]\right\}', \tag{5.11}$$

where a prime denotes differentiation with respect to η. The boundary conditions are,

$$\begin{aligned} &\text{on } \eta = 0: \quad c = 1 + \lambda\bar{k}(1-\phi)\left(-\frac{1}{\phi}\phi' - 1\right), \\ &\qquad\qquad \phi = \phi_0; \\ &\text{as } \eta \to \infty, \quad \phi \to \phi_\infty, \end{aligned} \tag{5.12}$$

where ϕ_∞ is determined by matching to (5.8) or (5.9) on $\xi = c$, thus (for $m \gg 1$)

$$\phi_\infty/\phi_0 \approx (\phi_0 c/m\lambda)^{1/(m-1)}. \tag{5.13}$$

Integrating, we have

$$c(\phi - \phi_0) = \lambda\bar{k}(1-\phi)^2\left(\frac{1}{\phi}\phi' + 1\right) - (1-c)(1-\phi_0), \tag{5.14}$$

whose solution can be written as a quadrature. In particular, we require $\phi \to \phi_\infty$, $\phi' \to 0$ as $\eta \to \infty$ thus

$$c(\phi_0 - \phi_\infty) = -\lambda(1-\phi_\infty)^2(\phi_\infty/\phi_0)^m + (1-c)(1-\phi_0). \tag{5.15}$$

The equations (5.13) and (5.15) determine c and ϕ_∞. They can be simplified when $m \gg 1$, and we obtain

$$c \approx \frac{1-\phi_0}{1-\phi_\infty}. \tag{5.16}$$

For the special case of $\lambda = 100$, $m = 8$ and $\phi_0 = 0.5$, matching (5.8) to (5.15) gives $\phi_\infty = 0.17177$ and $c = 0.58763$. As a specific illustration, Fig. 14 compares the numerically calculated ϕ versus Z profiles at $t = 20$ to the inner solution, (5.14), and to the outer solution, (5.8), and its explicit approximation, (5.9). There is good agreement between the boundary layer solution for $0.8 < Z \leq 1$ and the full numerical solution. In addition, the matched outer solution, (5.8) is in reasonable agreement with the numerical solution for $0.1 < Z < 0.75$. The consistency between the calculated values and the asymptotic approximations serve to validate the numerical technique used to solve the non-linear diffusion equation for ϕ.

5.1.2 $\lambda \ll 1$

For $z \sim 1$ and $\lambda \ll 1$, (5.2) is approximately $\phi_z \approx 0$, with $\phi[h(t)] = \phi_0$, hence

$$\phi \approx \phi_0. \tag{5.17}$$

As we see in Figs 11 and 12, there is a boundary layer at the base which varies with time. Its description is recovered as follows. Put

$$t = \tau/\lambda, \tag{5.18}$$

so that for $\tau = O(1)$ (or just $\tau \gg \lambda$), we have $h \gg 1$, and near the base, the problem for ϕ is

$$\phi_\tau = \frac{\partial}{\partial z}\left\{\bar{k}(1-\phi)^2\left[\frac{1}{\phi}\frac{\partial\phi}{\partial z} - 1\right]\right\} \tag{5.19}$$

with

$$\begin{aligned} &\phi_z - \phi = 0 \text{ on } z = 0, \\ &\phi \to \phi_0 \text{ as } z \to \infty. \end{aligned} \tag{5.20}$$

The latter condition above is the matching condition to the far field, and assumes $z \ll h$. Since $h \sim t$, this is equivalent to $z \ll \tau/\lambda$. Integrating (5.19) from $z = 0$ to ∞, we have

$$\frac{d}{d\tau}\int_0^\infty (\phi_0 - \phi)\, dz = (1-\phi_0)^2. \tag{5.21}$$

The equation (5.19) with boundary conditions (5.20) admits a local similarity solution. The similarity variable is $z/\sqrt{\tau}$, so that $z \ll \tau/\lambda$ if $\sqrt{\tau} \gg \lambda$, i.e. $t \gg \lambda$. Thus the similarity solution may be valid for times of order one. In keeping with (5.21), since $z \sim \sqrt{\tau}$, we expect $\phi_0 - \phi \sim \sqrt{\tau}$ (since $\int(\phi_0 - \phi)\, dz \sim \tau$), and thus we seek a *local* similarity solution in the form of a power series in $z/\sqrt{\tau}$ and τ. Specifically, we put

$$\phi = \phi_0 - \tau^{1/2}\psi(\zeta) + \tau\phi_2(\zeta) + \cdots, \quad \zeta = \frac{z}{2(1-\phi_0)}\sqrt{\frac{\phi_0}{\tau}}; \tag{5.22}$$

substituting this expression into (5.19) and equating powers of τ leads to a first approximation for ψ:

$$\psi'' + 2\zeta\psi' - 2\psi = 0, \tag{5.23}$$

with a solution satisfying the boundary condition at infinity,

$$\psi = A\int_\zeta^\infty (u - \zeta)e^{-u^2}\, du. \tag{5.24}$$

On $\zeta = 0$, we require $\tau^{1/2}\psi_z = -\phi_0$, i.e. $\psi_\zeta = -2(1-\phi_0)\phi_0^{1/2}$, whence

$$A = 4(1-\phi_0)(\phi_0/\pi)^{1/2}. \tag{5.25}$$

Finally,

$$\phi \approx \phi_0 - 4(1-\phi_0)(\phi_0\tau/\pi)^{1/2} \times \int_{z/2(1-\phi_0)\sqrt{\phi_0/\tau}}^\infty \left[u - \frac{z}{2(1-\phi_0)}\sqrt{\frac{\phi_0}{\tau}}\right] e^{-u^2}\, du. \tag{5.26}$$

This is consistent with Fig. 11, which shows the same algebraic increase in $\phi_0 - \phi$ as τ increases. In Fig. 15, we compare $\psi(\zeta)$ to the numerical solution at $t = 1$ and 10 for the case of $\lambda = 0.01$. The results show that for small times, there is good qualitative agreement between the similarity solution and the calculated values for ϕ. For larger values of t, the calculated values of $(\phi_0 - \phi)/\sqrt{\tau}$ deviate more from ψ. Since the expansion in (5.22) is accurate to $O(\sqrt{\tau})$, one expects the deviation between the similarity solution and the numerical results to increase with t. At $t = 1$, the difference between ψ and the numerical value at $\zeta = 0$ is 0.04 and for $t = 10$, the difference is 0.08, which shows that the deviations are indeed bounded by $\sqrt{\tau}$.

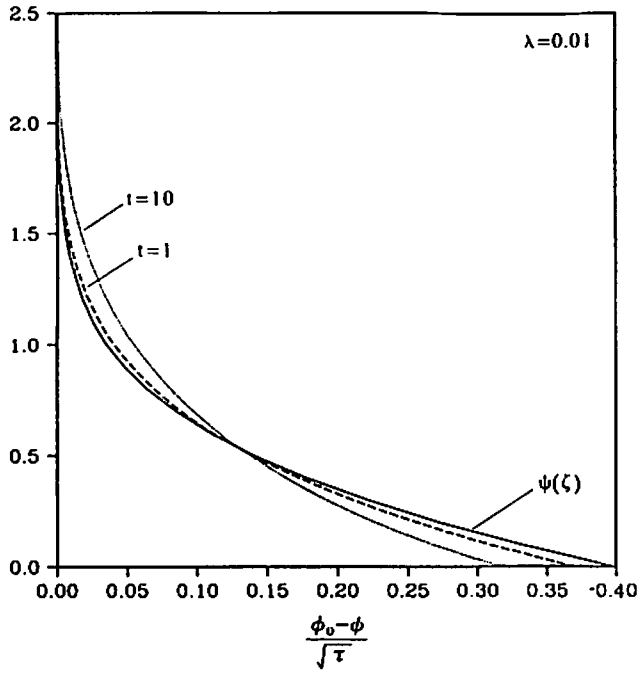

Figure 15. A comparison of the numerically calculated porosity profile to the similarity solution $\psi(\zeta)$ (solid line) for the case of $\lambda = 0.01$. The numerical solution is shown for $t = 1$ (dashed line) and for $t = 10$ (dotted line). The abscissa is the rescaled porosity and the ordinate is the similarity variable ζ as defined in the text, (5.22).

6 CONCLUSIONS

The literature on the modelling of compaction is not a huge one, despite its importance in understanding the behaviour of sedimentary basins. We have outlined a framework within which a very general model for compaction may be constructed, which potentially includes prescription of the motion of four separate phases, namely free pore water, montmorillonite, illite and quartz. It is possible to include a description of diagenesis and a very general rheology. In particular, we have suggested that a porosity–effective pressure relationship such as is implicit in Athy's law is a necessary constituent of any rheological law, though whether it need be akin to Athy's law is a moot point. In addition, we suggest that effective pressure may be properly given by an expression (Skempton 1960) of the form

$$p_e = P - (1 - a)p, \tag{6.1}$$

where a is the specific grain contact area. While $a \to 0$ may be appropriate for soils and unconsolidated sandstones, it is not at all obvious that this will remain true for rocks at high pressure, particularly when cementation and pressure solution occur. If $a \neq 0$, but is constant, there is little effect on numerical solutions, but in reality a may depend on p_e and ϕ_s, for example.

In this paper, we have concentrated on the simplest model for compaction, which omits diagenesis entirely. This model can be explicity collapsed to a single, non-linear diffusion equation for the porosity ϕ with a free boundary which is determined by a kinematic condition involving the sedimentation rate.

As such, this model is essentially that of Smith (1971), yet to our knowledge a methodical study of it has never been carried out. We have shown that the dynamical behaviour depends significantly on a single dimensionless parameter λ, which is a measure of the ratio of the sedimentation time-scale to the Darcy-flow time-scale; thus $\lambda \gg 1$ means high permeability or low sedimentation rate; $\lambda \ll 1$ means low permeability or high sedimentation rate; and for values of (unconsolidated) permeability of $10^{-19}\,\mathrm{m}^2$, and a sedimentation rate of $150\,\mathrm{m\,Ma}^{-1}$, we find $\lambda \approx 10$. Values of $\lambda > 1$ are therefore of interest, though $\lambda \ll 1$ may also be, in certain circumstances.

We have found two distinctive kinds of behaviour. When $\lambda > 1$, solutions for ϕ behave as in Fig. 5. Sedimentation is sufficiently slow that compaction occurs in a layer of thickness $O(1)$ at the top surface. Below this, there is a region of 'abyssal' porosity, where, if the permeability exponent m is large, then (from 5.9) $\phi \approx \phi_0(\phi_0/m\lambda)^{1/(m-1)}$. On the other hand, if $\lambda \ll 1$, then solutions are exemplified by Fig. 11. Sedimentation is so rapid that compaction occurs in a layer at the basement, whose thickness grows proportionally to $t^{1/2}$.

A hydrostatic pore pressure corresponds to $\partial p/\partial z = -r$; more precisely, the overburden, hydrostatic and excess pore pressures $P, p_h, \Pi = p - p_h$ (all dimensionless) are easily found from (4.30) to satisfy

$$\begin{aligned} -\frac{\partial P}{\partial z} &= (1-\phi) + r, \\ -\frac{\partial p_h}{\partial z} &= r, \\ \frac{\partial \Pi}{\partial z} &= (1-\phi)(1-\phi_z/\phi), \end{aligned} \tag{6.2}$$

thus, an excess pore pressure gradient develops when $\phi - \phi_z > 0$.

In the slowly sedimenting case, $\lambda > 1$, overpressuring occurs at large times, since for $z \gg 1$ (see 5.9), $\phi_z \ll \phi$, so that

$$-\frac{\partial \Pi}{\partial z} \approx 1 - \phi. \tag{6.3}$$

The reason is that, for sufficiently large times (and *any* λ), ϕ will decrease enough to cause $\lambda \bar{k} < 1$, and pore fluid becomes trapped. Possibly more relevant is what happens for $z, t \sim 1$ with $\lambda \gg 1$; then, writing (5.2) in the form

$$\phi_t = \lambda \frac{\partial}{\partial z}\left\{\bar{k}(1-\phi)\left[-\frac{\partial \Pi}{\partial z}\right]\right\}, \tag{6.4}$$

we see that $\partial\Pi/\partial z = O(1/\lambda)$, and overpressuring does not occur, as can be expected.

For the case of rapid sedimentation, we again have (6.3), in fact

$$\Pi \approx (1 - \phi_0)(h - z), \tag{6.5}$$

and the pore fluid is overpressured. This is true even for $z, t \sim 1$, since with $\lambda \ll 1$, $\phi_t \approx O(\lambda)$, whence $\phi \approx \phi_0$ and (6.5) still applies. These conclusions are consistent with expectation, and shed no light on the formation of seals, the study of which requires a more sophisticated model.

ACKNOWLEDGMENTS

This work forms part of an NERC-funded research project on 'Compaction in Sedimentary Basins' under the direction of Professor Desmond McConnell, FRS, which supports the research of both authors. We thank Chris Noon, Desmond McConnell, Mervyn Jones, Mike Leddra, Keith Refson, Dave Scott and Neil Skipper for discussion. Courtney Coleman kindly provided copies of the Claremont Mathematics Clinic reports on overpressuring.

REFERENCES

Athy, L. F., 1930. Density, porosity, and compaction of sedimentary rocks, *Am. Ass. Petrol. Geol. Bull.*, **14**, 1–22.

Atkinson, J. H. & Bransby, P. L., 1978. *The Mechanics of Soils: An Introduction to Critical State Soil Mechanics*, McGraw-Hill, New York.

Bethke, C. M., 1985. A numerical model of compaction-driven groundwater flow and heat transfer and its application to the paleohydrology of intracratonic sedimentary basins, *J. geophys. Res.*, **90**, 6817–1828.

Bethke, C. M., 1988. Reply to Palciauskas 1988, *J. geophys. Res.*, **93**, 3500–3504.

Bethke, C. M. & Corbet, F., 1988. Linear and nonlinear solutions for one-dimensional compaction flow in sedimentary basins, *Water Res. Res.*, **24**, 461–467.

Biedenweg, R., Byington, C., Kim, E., Mo, E., Oliver, D. & Coleman, C., 1975. Abnormally high pressures in sedimentary basins, *Interim report to Chevron Oil Field Research Company*, Claremont Graduate School, Claremont, CA.

Biot, M. A., 1941. General theory of three-dimensional consolidation, *J. appl. Phys.*, **12**, 155–164.

Bishop, R. S., 1979. Calculated compaction states of thick abnormally pressured shales, *Am. Ass. Petrol. Geol. Bull.*, **63**, 918–933.

Bredehoeft, J. D. & Hanshaw, B. B., 1968. On the maintenance of anomalous fluid pressures: I. Thick sedimentary sequences, *Geol. Soc. Am. Bull.*, **79**, 1097–1106.

Burland, J. B., 1990. On the compressibility and shear strength of natural clays, *Géotechnique*, **40**, 329–378.

Chen, W. F. & Mizuno, E., 1990. *Nonlinear Analysis in Soil Mechanics: Theory and Implementation*, Elsevier.

Drew, D. A., 1983. Mathematical modelling of two-phase flow, *A. Rev. Fluid Mech.*, **15**, 261–291.

Drew, D. A. & Wood, R. T., 1985. Overview and taxonomy of models and methods, *Workshop on two-phase flow fundamentals, National Bureau of Standards*, Gaithersburg, MD, Sept. 22–27, 1983, 88 pp.

Fowler, A.C., 1990. A compaction model for melt transport in the Earth's asthenosphere. Part I: the basic model, in *Magma Transport and Storage*, pp. 3–14, ed. Ryan, M. P., John Wiley.

Gibson, R. E., 1958. The progress of consolidation in a clay layer increasing in thickness with time, *Géotechnique*, **8**, 171–182.

Hanshaw, B. B. & Bredehoeft, J. D., 1968. On the maintenance of anomalous fluid pressures: II. Source layer at depth, *Geol. Soc. Am. Bull.*, **79**, 1107–1122.

Hunt, J. M., 1990. Generation and migration of petroleum from abnormally pressured fluid compartments, *Am. Ass. Petrol. Geol. Bull.*, **74**, 1–12.

Keith, L. A. & Rimstidt, J. D., 1985. A numerical compaction model of overpressuring in shales, *Math. Geol.*, **17**, 115–135.

Lambert, P., Muntean, M., Coleman, C., Noe, T. & Larson, D. A., 1979. A mathematical model of fluid pressure variation and other geophysical phenomena in a sedimentary basin, *Final report to Chevron Oil Field Research Company*, Claremont Graduate School, CA.

Palciauskas, V. V., 1988. Comment on 'A numerical model of compaction-driven groundwater flow and heat transfer and its application to the paleohydrology of intracratonic sedimentary basins' by Craig M. Bethke, *J. geophys. Res.*, **93**, 3497–3499.

Rubey, W. W. & Hubbert, M. K., 1959. Role of fluid pressure in mechanics of over-thrust faulting; II. Overthrust belt in geosynclinal area of western Wyoming in light of fluid-pressure hypothesis, *Bull. Geol. Soc. Am.*, **70**, 167–206.

Schiffman, R. L., Pane, V. & Gibson, R. E., 1984. The theory of one-dimensional consolidation of saturated clays; IV. An overview of nonlinear finite strain sedimentation and consolidation, in Sedimentation/Consolidation Models, *ASCE Conference*, pp. 1–29, eds Yong, R. N. & Townsend, F. C.

Schofield, A. N. & Wroth, C. P., 1986. *Critical State Soil Mechanics*, McGraw-Hill, New York.

Sharp, J. M., Jr, 1976. Momentum and energy balance equations for compacting sediments, *Math. Geol.*, **8**, 305–322.

Sharp, J. M., Jr, 1983. Permeability controls on aquathermal pressuring, *Am. Ass. Petrol. Geol. Bull.*, **67**, 2057–2061.

Sharp, J. M., Jr & Domenico, P. A., 1976. Energy transport in thick sequences of compacting sediment, *Geol. Soc. Am. Bull.*, **87**, 390–400.

Skempton, A. W., 1960. Effective stress in soils, concrete and rocks, in *Pore Pressure and Suction in Soils*, Butterworths, London.

Smith, J. E., 1971. The dynamics of shale compaction and evolution in pore–fluid pressures, *Math. Geol.* **3**, 239–263.

Terzaghi, K., 1936. The shearing resistance of saturated soil and the angle between the planes of shear, *Proc. Ist Int. Conf. Soil Mech. and Foundn Engng*, vol 1, pp. 54–56, Harvard, MA.